Title: Impact of long-term rapamycin treatment on age-related osteoarthritis in common marmoset

Authors: Dennis M. Minton[1], Aditya R. Ailiani[1], Michael D.K. Focht[2], Mariana E. Kersh[2,3,4], Angela J. Marolf[5], Kelly S Santangelo[6], Adam B. Salmon[7,8,9], Adam R. Konopka[1].

[1]Division of Geriatrics and Gerontology, Department of Medicine, University of Wisconsin-Madison, Madison, Wisconsin, USA.
[2]Department of Mechanical Science and Engineering, University of Illinois Urbana-Champaign, Champaign, IL, USA.
[3]Carle Illinois College of Medicine, University of Illinois Urbana-Champaign, Champaign, IL, USA.
[45]Beckman Institute for Advanced Science and Technology, University of Illinois Urbana-Champaign, Champaign, IL, USA.
[5]Department of Veterinary Clinical Sciences, Ohio State University, Columbus, OH, USA.
[6]Department of Microbiology, Immunology, and Pathology, College of Veterinary Medicine and Biomedical Sciences, Colorado State University, Fort Collins, CO, USA.
[7]Barshop Institute for Longevity and Aging Studies, San Antonio, TX, USA.
[9]Department of Molecular Medicine, University of Texas Health San Antonio, San Antonio, TX, USA.
[10]Geriatric Research, Education, and Clinical Center, South Texas Veterans Healthcare System, San Antonio, TX, USA.

Running Title: Rapamycin does not modify age-related OA

Corresponding Author:

Adam R. Konopka, PhD
Division of Geriatrics and Gerontology
Department of Medicine
University of Wisconsin-Madison
akonopka@medicine.wisc.edu

Abstract

Objective: Pharmacologic inhibition of the mechanistic target of rapamycin (mTOR) can attenuate experimental osteoarthritis (OA) in young, male preclinical models. However, the potential of mTOR inhibition as a therapeutic mechanism for OA remains unknown. The goal of this study was to determine if mTOR-inhibition by oral rapamycin can modify OA pathology in the common marmoset, a translational model of age-associated OA.

Methods: microCT and histopathologic assessments of the knee were performed on formalin-fixed hindlimbs obtained from common marmosets treated with oral rapamycin (n=24; 1mg/kg/day) or parallel control group (n=41). Rapamycin started at 9.2±3.0 years old and lasted until death (2.1±1.5 years). In a subset of marmosets, contralateral hind limbs were collected to determine mTOR signaling in several joint tissues.

Results: Rapamycin decreased P-RPS6$^{Ser235/36}$ and increased P-Akt2^{Ser473} in cartilage, meniscus, and infrapatellar fat pad, suggesting inhibition of mTORC1 but not mTORC2 signaling. Rapamycin-treated marmosets had lower lateral synovium score versus control but there was no difference in the age-related increase in microCT or cartilage OA scores. Subchondral bone thickness and thickness variability were not different with age but were lower in rapamycin-treated geriatric marmosets, which was largely driven by females. Rapamycin also tended to worsen age-related meniscus calcification in female marmosets.

Conclusion: Oral rapamycin attenuated mTORC1 signaling and may have caused feedback activation of mTORC2 signaling in joint tissues. Despite modifying site-specific aspects of synovitis, rapamycin did not modify the age-associated increase in OA in geriatric marmosets. Conversely, rapamycin may have had deleterious effects on meniscus calcification and lateral tibia subchondral bone, primarily in geriatric female marmosets.

Introduction

Increasing age is the greatest risk factor for osteoarthritis (OA). OA further increases the age-related risk of multi-morbidity. With no available disease modifying therapies for OA, the economic and societal impacts of OA are expected to rapidly inflate with population aging. A critical barrier to the development of disease modifying therapies for human OA is a lack of models that faithfully recapitulate human OA. Recently, we found that the smallest anthropoid non-human primate, the common marmoset, replicates most aspects of human joint tissue organization and develops hallmark OA pathologies in a similar age-related fashion to humans (1). Therefore, the marmoset represents an advantageous model to translate OA therapeutics from rodents to humans.

The mechanistic target of rapamycin (mTOR) is a nutrient- and growth-factor-sensitive protein kinase that exists as two distinct complexes, mTORC1 and mTORC2. Phosphorylated mTORC1/2 substrates are abundant in OA cartilage from humans, dogs, and rodents (2–5). Phosphorylation of downstream substrates of mTORC1 (5) and mTORC2 (3) can induce and exacerbate OA in mice, while cartilage specific knockout of the entire mTOR protein kinase effectively protects against surgically induced knee OA pathology in young male mice (4). These data indicate that mTOR inhibition may have therapeutic potential for OA.

Pharmacological inhibition of mTORC1 signaling by rapamycin delays several age-related pathologies and extends lifespan in multiple model systems (6). Similarly, systemic or intra-articular treatment with rapamycin can attenuate experimentally induced OA in young, male rodents (2,7). However, this is equivocal as we and others have found worsened OA pathology after rapamycin treatment (8,9). Importantly, it remains unknown whether rapamycin can modify naturally occurring OA in older male and female subjects. Therefore, to determine if mTOR-inhibition by rapamycin can impact age-related OA in a translational model of OA, we analyzed knee joints obtained from common marmosets that received long-term oral rapamycin starting near mid-life or served as controls.

Materials and Methods

Animal Use and Tissue Collection

Common marmosets were housed and maintained using previously published husbandry guidelines at the Barshop Institute for Longevity and Aging Research at UT Health San Antonio until natural death or compassion euthanasia. At necropsy, hind limbs were either fixed in formalin (n=64) or frozen (n=19) and shipped to University of Wisconsin-Madison (1).

Statistical Analysis

To evaluate the effect of Rapamycin-treatment, sex, and age, multiple linear regression models were used with main effects, 2-way interactions, and 3-way interactions. If residuals were non-normally distributed as assessed by the Kolmogorov-Smirnov test, data were square-root transformed. If square-root transformation failed to normalize residuals, data were rank-transformed. Unpaired t-tests or Mann-Whitney tests were used for pairwise comparisons between treatment groups for pooled sexes, males, and females, depending on normality of data as assessed by the Kolmogorov-Smirnov test. Because marmosets are considered 'aged' at 8-years-old, we previously stratified into 'adult' (<8-years) and 'geriatric' (>8-years) for grouped analysis. Due to low number of 'adult' rapamycin-treated marmosets, we assessed treatment effects pairwise in geriatric marmosets only. P-values ≤ 0.05 were considered statistically significant.

Methods regarding rapamycin treatment, radiographic, histological, and molecular outcomes are described in **Supplementary Methods.**

Results

Rapamycin treatment duration and physical characteristics.

Average treatment durations for marmosets pooled and stratified by age-group and sex are shown in **Table S1**. On average, marmosets were treated with rapamycin for 2.1±1.5 years. Peak body mass, lean and fat mass, blood glucose, LDL cholesterol, and triglyceride levels were also measured on a subset of marmosets as shown in **Table S2** and were not significantly different between control and rapamycin.

Molecular target engagement in joint tissues.

Representative blots and mTOR signaling data from articular cartilage, meniscus, and infrapatellar fat pad are presented in **Figure 1A-I**. Rapamycin attenuated p-RPS6$^{Ser235/36}$ ($P<0.05$) by ~50% versus control in cartilage, meniscus, and fat pad. Rapamycin did not affect p-Akt1^{Ser473} but increased p-Akt2^{Ser473} 2-fold versus control in cartilage ($P<0.01$), meniscus ($P=0.07$), and fat pad ($P<0.01$).

Rapamycin did not modify radiographic OA score or cartilage pathology.

Total uCT OA score (**Figure S1A-D**) increased with age in both sexes but was not different in rapamycin-treated vs. control marmosets. Cartilage pathology (**Table S3**, **Figure S2A-H**) increased with age and manifested more severely in geriatric females but was not different in rapamycin-treated vs. control marmosets.

Synovial pathology scores were lower in rapamycin-treated marmosets.

Total synovial score for the lateral compartment was lower in rapamycin-treated marmosets when sexes were pooled (**Figure S3A**, $P<0.05$). There were no differences between control and rapamycin-treated marmosets for the individual scoring criteria of pannus infiltration, synovial hyperplasia, or sub-synovial inflammation (**Figure S3B-D**); however, synovial fibrosis scores were lower in the medial compartment of rapamycin-treated males vs. male controls (**Figure S3E**).

Greater meniscus calcification in rapamycin-treated geriatric marmosets.

Medial meniscus volume was predicted by multiple regression model (**Figure 2A**; $R^2=0.50$, $P<0.0001$). Age ($P=0.002$) was a significant main effect predictor with a trend for sex ($P=0.08$). Interaction effects were found for age and sex ($P=0.02$) and a trend for sex and treatment ($P=0.08$), reflective of more rapamycin treated geriatric female with severe calcification. When geriatric marmosets were pooled and stratified by sex, no significant treatment effects were found (**Figure 2B**) despite rapamycin-treated geriatric marmosets having ~2-fold higher meniscus calcification volume than controls. No effects of age, sex, or treatment were seen in the lateral meniscus (data not shown).

Rapamycin treated marmosets displayed altered subchondral bone architecture.

Results of multiple regression models for cortical and trabecular bone parameters are contained in **Table S3** and **Table S4**, respectively. Lateral tibia trabecular thickness was lower in

rapamycin-treated marmosets, and medial (P=0.002) and lateral (P=0.05) femoral trabecular bone mineral density was predicted by increasing age.

When stratifying by age-groups, the lateral tibia emerged as a site with consistent rapamycin effect. Composite lateral tibia subchondral cortical thickness heatmaps for control and rapamycin-treated marmosets are shown in **Figure 3A**. In geriatric marmosets pooled for sex, rapamycin-treated marmosets had lower mean (**Figure 3B**), max (**Figure 3C**), and standard deviation (**Figure 3D**) of cortical thickness in the lateral tibia versus controls. This may have been driven by females, as rapamycin-treated females displayed lower (P=0.02) standard deviation and non-significant trends for lower mean (P=0.09) and max (P=0.06) cortical thickness.

Trabecular thickness in the lateral tibia (**Figure 3E**, P=0.02) and lateral femur (**Figure 3F**, P=0.004) were both lower in rapamycin-treated marmosets than controls when sexes were pooled. Trabecular thickness in the lateral femur was lower ($P \leq 0.05$) in rapamycin-treated males and females compared to their respective controls. No treatment effects were seen for cortical or trabecular thickness or density for any other joint compartment (data not shown).

Discussion

The objective of this study was to examine the impact of mTOR inhibition by oral rapamycin on age-related OA pathology in common marmosets. We found that rapamycin attenuated the phosphorylation of mTORC1 substrate $RPS6^{Ser235/36}$ and induced activation of the mTORC2 substrate $Akt2^{Ser473}$ in multiple joint tissues. Approximately 2-years of rapamycin treatment initiated near median lifespan did not modify the age-related increase in radiographic or cartilage histopathologic OA scores but may have decreased aspects of synovitis. However, in female geriatric marmosets receiving rapamycin, medial meniscus calcification appeared to be more severe and lateral tibia subchondral cortical thickness and thickness variability were lower versus control. These effects may be maladaptive, as meniscal calcification occurs during aging and OA, and the decrease in subchondral bone thickness in the lateral tibia does not combat changes during age-associated OA. Collectively, these data indicate that mTORC1 inhibition in joint tissues by daily, oral rapamycin may lower select indices of age-related synovitis but does not offer benefits on other hallmarks of OA and may have deleterious effects on meniscus calcification and subchondral bone remodeling.

Upregulation of mTOR signaling during OA is conserved across multiple species including humans (4). Genetic deletion of the entire mTOR kinase had the strongest protective effects against surgically induced OA (4). However, the impact of pharmacological mTOR-inhibition by rapamycin on OA have been equivocal (4,5,7–9). In the present study, oral rapamycin attenuated mTORC1 and increased mTORC2 signaling as estimated by phosphorylation of downstream substrates in articular cartilage, meniscus, and infrapatellar fat pad, and did not modify radiographic or cartilage histopathologic OA scores. We have previously shown in male Dunkin-Hartley guinea pigs, dietary rapamycin (14ppm) with or without metformin (±1000ppm) decreased mTORC1 but increased mTORC2 signaling when all rapamycin-treated animals were retrospectively pooled, and this was accompanied by worsened OA pathology (9). Collectively, our data in marmosets and guinea pigs are consistent with findings that acute mTORC1 inhibition can alleviate negative feedback on upstream receptor tyrosine kinases and increase signal through mTORC2/Akt (6), which is consistent with short joint-space residence times of small drug compounds and therapeutics (1-4h) (10). Further, since constitutively activated Akt signaling can induce and worsen experimental OA in mice (3), it is plausible that increased Akt phosphorylation in rapamycin-treated marmosets may have negated any protective effects mTORC1 inhibition on age-related OA. Future work is needed to determine if inhibition of both mTORC1 and mTORC2 signaling within the joint space is needed to achieve therapeutic efficacy.

The age-related increase in medial meniscus calcification tended to be more severe in geriatric marmosets receiving rapamycin, which appeared to be driven by geriatric females. During OA, the menisci can degenerate, become calcified, and secrete inflammatory cytokines which can exacerbate OA progression. Longitudinal human data from the Multicenter Osteoarthritis Study indicate that meniscus calcification is associated with severity and progression of pain (11). While pain was not measured in the present study as originally planned due to COVID-19 restrictions, previous reports indicate an age-related increase in pain behavior linked to OA in mice and predictive of mortality in marmosets (12). The role of mTOR in meniscal calcification is not well characterized; however, mTOR inhibition by rapamycin increased calcification in bone marrow mesenchymal stem cells *in vitro* and enhanced rat mandibular trabecular bone formation during inflammatory induction with lipopolysaccharides (13). These

data would support the notion that mTORC1 inhibition within a pro-inflammatory environment, as commonly seen during OA, may create a condition prone to osteogenesis and aberrant calcification.

Subchondral sclerosis is a hallmark observation during OA and is used as part of the Kellgren-Lawrence system to diagnose human OA. Rapamycin-treated marmosets had lower subchondral cortical and/or trabecular bone thickness and thickness variability in the lateral tibia and femur. While this may be viewed as resistance to sclerotic bone formation during OA, there was no age-related subchondral thickening observed at this site. Therefore, this may be a maladaptive effect of rapamycin treatment. We and others have previously observed decreased bone mass after rapamycin treatment. 12-weeks of dietary rapamycin in Dunkin-Hartley guinea pigs decreased cortical thickness but also at other non-OA-affected sites (9). Further, rapamycin (4mg/kg every other day) decreased cortical and trabecular bone thickness and increased serum CTX-1 and other indices of bone resorption in 12-16-week-old female mice (14). Further, rapamycin (5mg/kg, intra-articular, daily) caused subchondral bone loss male Sprague-Dawley rats during a TMJ-OA model (8). Together, these data support rapamycin can decrease bone mass, though this may be dependent on age, disease status, and frequency of dosing.

Some characteristics of synovitis appear to be positively impacted by rapamycin. In the lateral joint compartment, total synovial scores and fibrosis scores were lower in rapamycin-treated marmosets when sexes were pooled and in males only, respectively. While these effects were not found in the medial compartment where OA manifests most severely, there is precedent that mTOR signaling contributes to synovitis. Macrophage infiltration and polarization via hyperactive mTORC1 signaling have been shown to promote synovitis and OA progression (15), and rapamycin treatment decreased synovitis in male mice following DMM (7).

While this is the first study to evaluate the effects of rapamycin on OA outcomes in non-human primates, we acknowledge some study limitations. As demonstrated in our previous study (1), age-related OA in marmosets manifests with a heterogenous onset and progression compared to post-traumatic OA models where there is a robust and controlled stimulus to induce OA. While this is common to primary OA in mice and humans, many of the marmosets likely had some amount of age and/or OA-related changes to joint tissues when the rapamycin treatment began. Because of the cross-sectional study design, we cannot account for existing OA burden at treatment start. Therefore, these findings may not be reflective of the potential preventative effects of mTOR inhibition on OA outcomes in subjects at high risk for developing OA (i.e., ACL rupture). Future work may seek to account for existing OA burden prior to treatment through in vivo imaging and/or OA biomarkers.

Due to the known kinetics of rapamycin on mTOR signaling in other cells and tissue types, our data align with the concept that systemic rapamycin treatment may have low entry into and/or short residence time within the joint space to acutely inhibit mTORC1 and stimulate mTORC2 signaling. Therefore, alternative strategies to extend rapamycin joint residence time should be investigated to determine if inhibiting both mTORC1 and mTORC2 specifically within the joint space may increase therapeutic efficacy and minimize risk for off-target systemic metabolic side-effects. Collectively, our findings demonstrate the effects of oral rapamycin may lower select characteristics of synovitis but may also contribute to deleterious effects on meniscus calcification and subchondral bone structure.

ACKNOWLEDGEMENTS

This work is supported by supported by NIH-NIA R21-AG067464 (to ARK), NIH-NIA R01-AG050797 (to ABS), the San Antonio Nathan Shock Center (P30-AG013319), and the San Antonio Claude D. Pepper Center (P30-AG044271). DMM is supported by NIH-NIA T32-AG000213. The Konopka Laboratory is also supported by NIH-NIA U01-AG076941, U01-AG081482, Impetus Longevity Grant by the Norn Group and Hevolution Foundation, and New Investigator Award from AFAR and Hevolution Foundation. μCT imaging was conducted at the Biomedical Imaging Center of the Beckman Institute for Advanced Science and Technology at the University of Illinois Urbana-Champaign. The Konopka Laboratory is also supported by startup and other funds from the University of Wisconsin-Madison School of Medicine and Public Health and Department of Medicine. The content is solely the responsibility of the authors and does not necessarily represent the official views of the NIH or the United States Government.

References

1. Minton DM, Ailiani AR, Focht MDK, Kersh ME, Marolf AJ, Santangelo KS, et al. The common marmoset as a translational model of age-related osteoarthritis. GeroScience 2024 Mar 11 [cited 2024 Mar 20]; Available from: https://doi.org/10.1007/s11357-024-01103-5

2. Takayama K, Kawakami Y, Kobayashi M, Greco N, Cummins JH, Matsushita T, et al. Local intra-articular injection of rapamycin delays articular cartilage degeneration in a murine model of osteoarthritis. Arthritis Res Ther. 2014 Nov 17;16(6):482.

3. Xie J, Lin J, Wei M, Teng Y, He Q, Yang G, et al. Sustained Akt signaling in articular chondrocytes causes osteoarthritis via oxidative stress-induced senescence in mice. Bone Res. 2019 Aug 5;7(1):1–9.

4. Zhang Y, Vasheghani F, Li Y hua, Blati M, Simeone K, Fahmi H, et al. Cartilage-specific deletion of mTOR upregulates autophagy and protects mice from osteoarthritis. Ann Rheum Dis. 2015 Jul;74(7):1432–40.

5. Zhang H, Wang H, Zeng C, Yan B, Ouyang J, Liu X, et al. mTORC1 activation downregulates FGFR3 and PTH/PTHrP receptor in articular chondrocytes to initiate osteoarthritis. Osteoarthritis Cartilage. 2017;25(6).

6. Simcox J, Lamming DW. The central moTOR of metabolism. Dev Cell. 2022 Mar 28;57(6):691–706.

7. Caramés B, Hasegawa A, Taniguchi N, Miyaki S, Blanco FJ, Lotz M. Autophagy activation by rapamycin reduces severity of experimental osteoarthritis. Ann Rheum Dis. 2012 Apr;71(4):575–81.

8. Li Y, Yang J, Liu Y, Yan X, Zhang Q, Chen J, et al. Inhibition of mTORC1 in the rat condyle subchondral bone aggravates osteoarthritis induced by the overly forward extension of the mandible. Am J Transl Res. 2021 Jan 15;13(1):270–85.

9. Minton DM, Elliehausen CJ, Javors MA, Santangelo KS, Konopka AR. Rapamycin-induced hyperglycemia is associated with exacerbated age-related osteoarthritis. Arthritis Res Ther. 2021 Dec;23(1):253.

10. Evans CH, Kraus VB, Setton LA. Progress in intra-articular therapy. Nat Rev Rheumatol. 2014 Jan;10(1):11–22.

11. Liew JW, Jarraya M, Guermazi A, Lynch J, Wang N, Rabasa G, et al. Relation of Intra-Articular Mineralization to Knee Pain in Knee Osteoarthritis: A Longitudinal Analysis in the MOST Study. Arthritis Rheumatol. 2023;75(12):2161–8.

12. Ross CN, Davis K, Dobek G, Tardif SD. Aging Phenotypes of Common Marmosets (Callithrix jacchus). J Aging Res. 2012;2012:567143.

13. Li X, Chang B, Wang B, Bu W, Zhao L, Liu J, et al. Rapamycin promotes osteogenesis under inflammatory conditions. Mol Med Rep. 2017 Dec 1;16(6):8923–9.

14. Martin SA, Riordan RT, Wang R, Yu Z, Aguirre-Burk AM, Wong CP, et al. Rapamycin impairs bone accrual in young adult mice independent of Nrf2. Exp Gerontol. 2021 Oct 15;154:111516.

15. Zhang H, Lin C, Zeng C, Wang Z, Wang H, Lu J, et al. Synovial macrophage M1 polarisation exacerbates experimental osteoarthritis partially through R-spondin-2. Ann Rheum Dis. 2018 Oct 1;77(10):1524–34.

Figure Legends

Figure 1: Rapamycin inhibits mTORC1 signaling in knee joint tissues. Representative western blot images from articular cartilage, meniscus, and infra-patellar fat pad tissues are shown for p-RPS6$^{Ser235/36}$ and total RPS6, or p-Akt^{Ser473} and total Akt, with Ponceau S presented as a loading control. **A**) p-RPS6 normalized to total RPS6 was decreased in articular cartilage of Rapamycin-treated marmosets. **B**) p-Akt1 normalized to total Akt was not affected by rapa, but **C**) p-Akt2 normalized to total Akt was higher in rapamycin-treated marmosets. **D**) p-RPS6 normalized total RPS6 was decreased in meniscus of rapamycin-treated marmosets. **F**) p-Akt1 normalized to total Akt was not affected by rapa, but **H**) p-Akt2 normalized to total Akt was higher in rapamycin-treated marmosets. **G**) p-RPS6 normalized total RPS6 was decreased in infra-patellar fat pad of rapamycin-treated marmosets. **H**) p-Akt1 normalized to total Akt was not affected by rapa, but **I**) p-Akt2 normalized to total Akt was higher in rapamycin-treated marmosets. Comparisons were made using either student's t-test Mann-Whiteny test, depending on normality of data. Data are shown as mean with individual data points. *P<0.05, **P<0.01.

Figure 2: Meniscus calcification is increased in geriatric and female marmosets receiving rapamycin. **A**) Medial meniscus calcification volumes are presented as a scatter plot against age and **B**) stratified by treatment group for pooled and stratified sexes. Significant findings from multiple linear regression (A) are shown beside. Pairwise comparisons were made using Mann-Whitney tests. Data are presented as mean with individual data points.

Figure 3: Subchondral bone architecture is altered by rapamycin treatment. **A**) Composite cortical thickness heatmaps from control and Rapamycin-treated marmosets, scalebar beneath. **B**) Mean, **C**) max, and **D**) standard deviation of lateral tibia cortical bone thickness were all lower in rapamycin-treated marmosets than controls. **E**) Trabecular thickness in the lateral tibia and **F**) lateral femur were also lower in Rapamycin-treated marmosets than controls. L=lateral, T=tibia, F=femur. Data are presented both pooled and stratified by sex. Treatment effects were assessed by unpaired t-tests or Mann-Whitney tests, depending on normality of data. Data are shown as mean with individual data points. *P<0.05, **P<0.01

Individual Tables and Figures

Figure 1

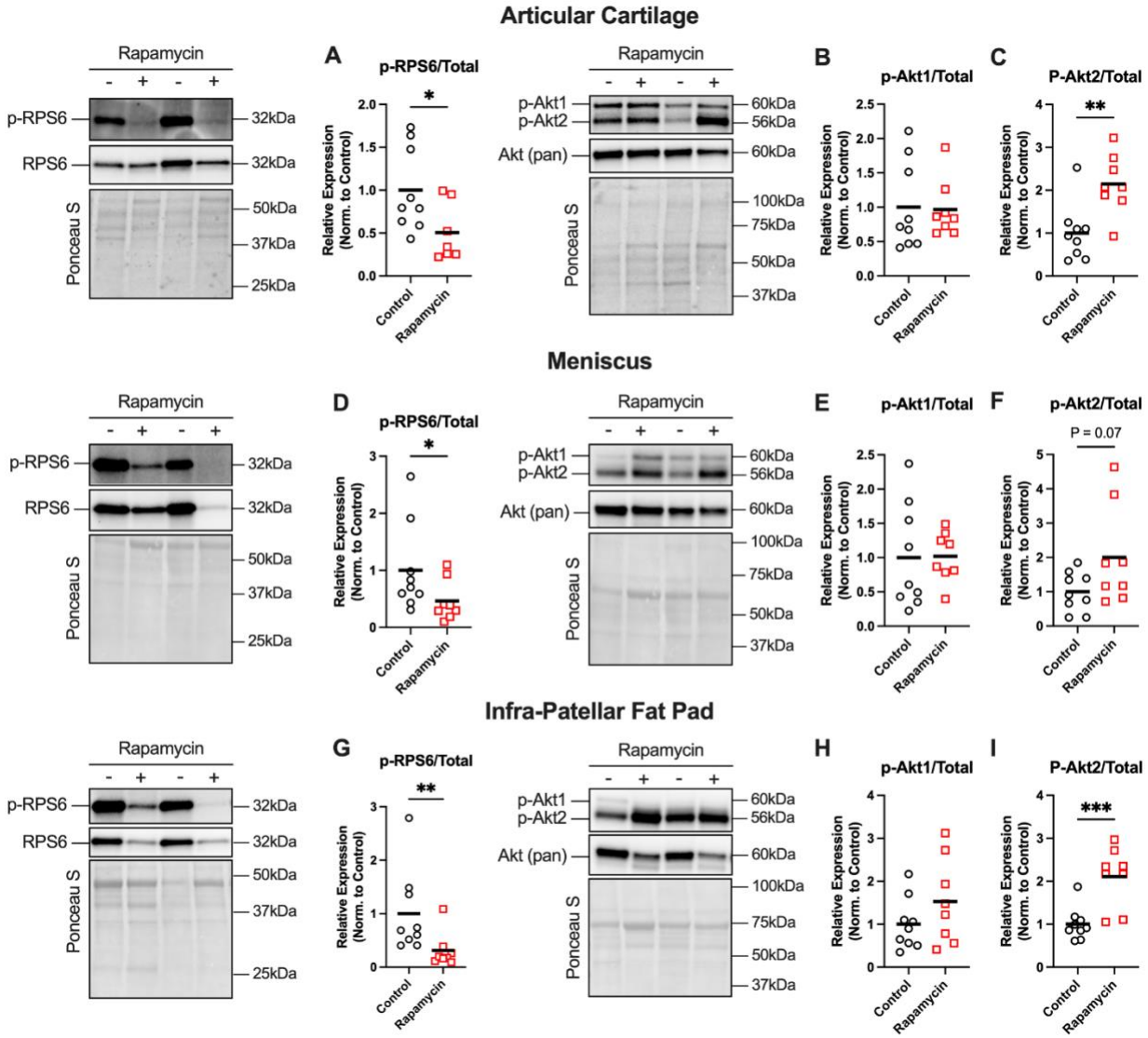

Figure 2

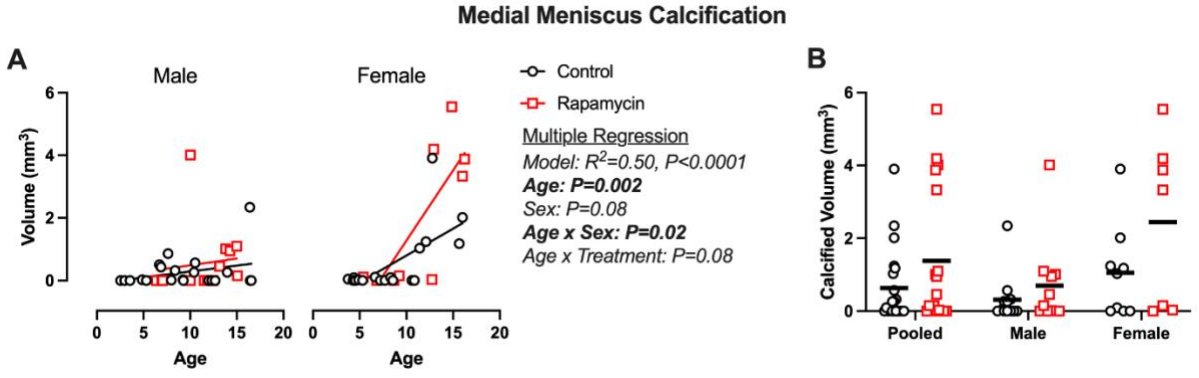
Medial Meniscus Calcification
A
Male
Female
Volume (mm³)
Age
Control
Rapamycin
Multiple Regression
Model: R²=0.50, P<0.0001
Age: P=0.002
Sex: P=0.08
Age x Sex: P=0.02
Age x Treatment: P=0.08
B
Calcified Volume (mm³)
Pooled
Male
Female

Figure 3

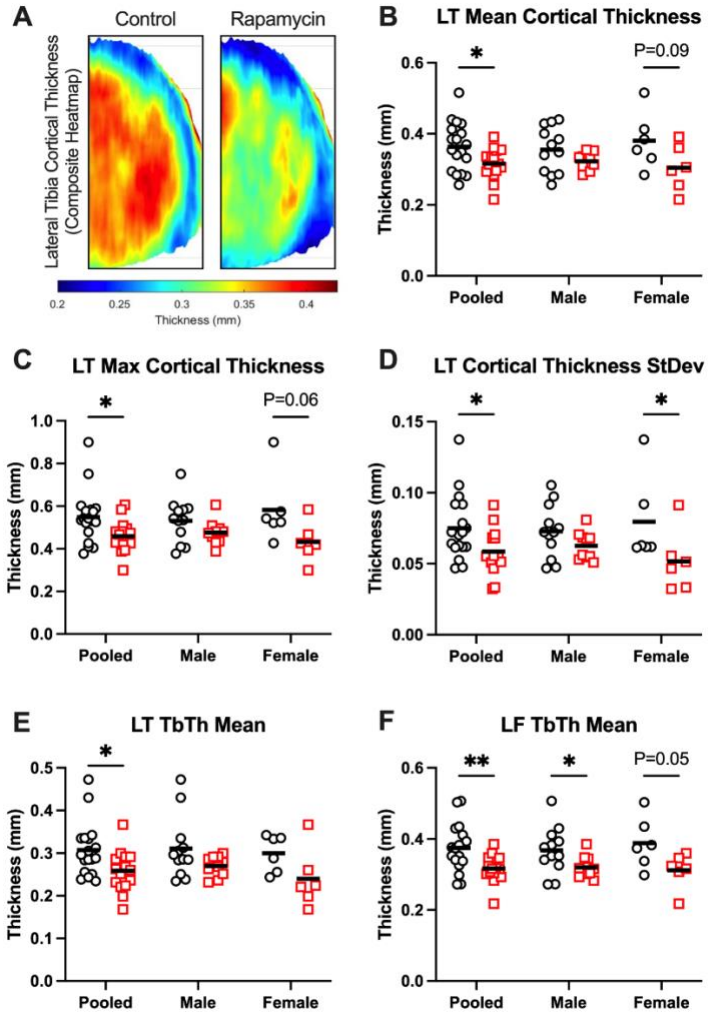
A
Control
Rapamycin
Lateral Tibia Cortical Thickness (Composite Heatmap)
0.2
0.25
0.3
0.35
0.4
Thickness (mm)
B
LT Mean Cortical Thickness
*
P=0.09
Thickness (mm)
Pooled
Male
Female
C
LT Max Cortical Thickness
*
P=0.06
Thickness (mm)
Pooled
Male
Female
D
LT Cortical Thickness StDev
*
*
Thickness (mm)
Pooled
Male
Female
E
LT TbTh Mean
*
Thickness (mm)
Pooled
Male
Female
F
LF TbTh Mean
**
*
P=0.05
Thickness (mm)
Pooled
Male
Female

Supplementary Information

METHODS

Rapamycin Treatment

Twenty-three (14M/9F) marmosets received eudragit-encapsulated rapamycin (1mg/kg/day) dissolved in yogurt. The control group consisted of 28 marmosets (14M/14F) that received yogurt vehicle with empty eudragit as previously published (1) and an additional 13 marmosets (7M/6F) from the general population that did not receive eudragit vehicle. All husbandry was identical and there were no differences in OA between the vehicle control and age-matched general population marmosets. Marmosets in the control group for this study were previously published to characterize OA pathology in the common marmoset (2). All samples were collected opportunistically at euthanasia determined by animals reaching veterinary end of life criteria.

Protein and RNA Extraction from Frozen Tissues

Frozen knee joints were thawed on ice for ~45-minutes and articular cartilage, menisci, and the infrapatellar fat pad were dissected and snap frozen until further processing. Tissues were placed in tubes containing 500uL Trizol (BRAND) and 500mg of 2.4mm ceramic beads and pulverized in an Omni Bead Ruptor (two 30-second cycles at 6m/s). RNA and protein were then extracted as previously described (3). RNA quantity and purity were evaluated via Nanodrop (Thermo), and protein concentration was quantified via bicinchoninic acid assay.

Western Blotting

Samples were prepared for western blotting as previously described (4). Equal amounts of protein were resolved on 4-15% TGX precast gels (BioRad) and transferred to nitrocellulose membranes (BioRad) and stained with Ponceau S to quantify total protein per lane. Membranes were blocked with 5% bovine serum albumin then incubated overnight at 4C with primary antibodies raised against p-RPS6 Ser235/236 (#4858), RPS6 (#2217), p-Akt Ser473 (#4060), and Akt (pan) (#4685) followed by an HRP-conjugated anti-Rabbit secondary antibody (#7074) for 45-min at room-temperature. All antibodies were from Cell Signaling (Danvers, MA, USA). Membranes were imaged using a BioRad Chemi-Doc after 5-min incubation in SuperSignal Femto chemiluminescent substrate (Thermo). Bands were quantified using densitometric analysis in ImageLab (BioRad).

All radiographic and histological analyses were performed as outlined in our previous manuscript (2), and all control and rapamycin-treated marmosets were processed and analyzed in parallel. Detailed methods can be found in our previous manuscript, however are replicated below for ease of readership:

microCT Acquisition and Quantitative Analysis

Knee joints were scanned while submerged in 70% ethanol using a Rigaku CT Lab GX130 at 120uA and 110kV for 14-minutes, achieving an isometric voxel size of 49um as previously performed (4). Three hydroxyapatite phantoms were included on each day of scanning to calculate bone mineral density.

For quantitative analysis, all scans were binarized using identical thresholds to allow for comparison across scans. In Amira (v2021.2, ThermoFisher), regions of calcified meniscus and were segmented, and volumes were quantified using the material statistics function. Representative 3D reconstructions were also created in Amira.

For analysis of subchondral bone, cortical and trabecular bone were separated using a previously validated algorithm (5). Three-dimensional thickness and density maps were created the ImageJ plug-in BoneJ. Articular surfaces were spatially normalized to account for morphological differences between marmosets, resulting in 81 subregions in the tibial plateaus and 40 subregions in the femoral condyles. For each sub-region, mean trabecular thickness and density were calculated. Subregions were then compiled to produce mean and max values for each joint compartment, as well as standard deviation as an index of heterogeneity of thickness and density across the articular surface. Three scans from the geriatric group could not be analyzed due to severe subchondral bone degeneration.

Semi-Quantitative microCT Scoring

To assess radiographic severity of OA, uCT scans were graded by a veterinary radiologist according to the criteria outlined in **Table S6** (6). Grading was performed in a single session utilizing standard transverse plane images and multiplanar reconstructions in sagittal and coronal planes while remaining blinded to marmoset age or sex. We also employed a semi-quantitative scoring system to evaluate calcification of the menisci. Briefly, the medial and lateral menisci were each assigned a score ranging from 0-5 depending on the size and frequency of ectopic calcification.

Histological Analysis

Following microCT scanning, knee joints were grossed of soft tissue, trimmed, and decalcified in 5% EDTA changed 2-3rx/week for 15-weeks or until fully decalcified by mechanical endpoint testing. Joints were then transected along the medial collateral ligament and processed for paraffin embedding. Sections were taken at 5-microns and stained with Toluidine Blue as previously described (2,4). In a blinded fashion, histological assessment of OA was performed using a grading scheme shown in **Table S7** which was adapted from the Modified Mankin guidelines for mice and other small rodents (7). Briefly, 3 sections across each joint compartment were graded in a blinded fashion for articular cartilage structural damage based on lesion depth and affected proportion of cartilage surface (0-11), tidemark duplication (0-3), proteoglycan loss as evident by loss of toluidine blue staining (0-8), and disruption of normal chondrocyte cellularity (0-4). Data were then presented as an average of the 3 scores. These criteria were assessed as individual phenomena and summed to produce a total histological score for each joint compartment and a whole-joint score.

Synovium Scoring

To assess OA-associated changes to the synovium/joint capsule, we employed a recently published scoring system developed to comprehensively evaluate histopathological changes in mouse models of OA (8). Scoring criteria are presented in **Table S8** but briefly included scores for pannus outgrowth and subsequent bone erosion, synovial exudate, synovial hyperplasia, sub-synovial inflammation, and scores for synovial fibrosis severity and coverage of fibrosis. Two mid-

joint coronal sections were stained with Hematoxylin & Eosin and used to produce a single score for the medial and lateral compartments for each marmoset. Synovial fibrosis severity and coverage were multiplied to produce the individual fibrosis score presented. To produce the total synovium score per compartment, all individual criteria were summed besides synovial fibrosis coverage to avoid over-representing fibrosis in the total score. Of note, some criteria are applied relative to cartilage thickness. We found marmoset cartilage to be substantially thicker than mouse, which may have decreased our ability to capture more subtle changes. However, the scoring system was still applied faithfully. Finally, because synovial exudate receives a binary score, it was not analyzed as an individual criteria but was included in the total score.

Tables and Figures

	Male		Female		Pooled Sexes	
	N	Duration (yrs)	N	Duration (yrs)	N	Duration (yrs)
Adult	3	0.6 ± 0.3	2	1.3 ± 0.3	5	0.9 ± 0.5
Geriatric	11	2.7 ± 1.6	8	2.2 ± 1.6	19	2.5 ± 1.6
Pooled Ages	14	2.2 ± 1.7	10	2.0 ± 1.4	24	2.1 ± 1.5

Table S1. Duration of rapamycin treatment in years for marmosets presented as pooled and stratified by age-group and sex. Number of marmosets is shown for each sub-group. Data are presented as mean ± SD.

Variable	Control	Rapamycin	P-value
Peak bodyweight (g)	446.6 ± 60.5	430.1 ± 54.2	0.36
Lean mass (g)	361.1 ± 46.2	351.8 ± 41.3	0.51
Fat mass (g)	32.0 ± 31.2	33.5 ± 20.9	0.82
Blood glucose (mg/dL)	161.3 ± 53.2	199 ± 81.2	0.15
LDL cholesterol (mg/dL)	161.0 ± 42.2	188.4 ± 49.6	0.14
Triglycerides (mg/dL)	187.6 ± 149.6	281.2 ± 169	0.14

Table S2: Peak bodyweight, lean mass, fat mass, blood glucose, LDL cholesterol, and triglycerides are shown for control and rapamycin-treated marmosets. Data are presented at mean ± SD. Treatment groups were compared using 2-tailed, unpaired t-tests and P-values are presented.

Variable		*Model Fit*		*Main Effects*			*2-way Interactions*			*3-way Interactions*
		R^2	P	Age	Sex	Treatment	Age x Sex	Age x Treatment	Sex x Treatment	Age x Sex x Treatment
Medial Tibia	CoTh Mean	0.06	0.86	P=0.46	P=0.96	P=0.60	P=0.77	P=0.69	P=0.50	P=0.63
	CoTh Max	0.18	0.15	P=0.09	P=0.56	P=0.10	P=0.48	P=0.12	P=0.59	P=0.68
	CoTh StDev	0.17	0.19	P=0.12	P=0.57	P=0.08	P=0.54	P=0.09	P=0.35	P=0.44
	CoBMD Mean	0.08	0.72	P=0.87	P=0.81	P=0.95	P=0.90	P=0.67	P=0.88	P=0.77
	CoBMD Max	0.06	0.85	P=0.90	P=0.86	P=0.96	P=0.98	P=0.83	P=0.96	P=0.96
	CoBMD StDev	0.16	0.24	P=0.08	P=0.38	P=0.41	P=0.23	P=0.25	P=0.59	P=0.70
Medial Femur	CoTh Mean	0.05	0.90	P=0.61	P=0.87	P=0.95	P=0.96	P>0.99	P=0.50	P=0.55
	CoTh Max	0.08	0.70	P=0.83	P=0.54	P=0.45	P=0.74	P=0.49	P=0.64	P=0.64
	CoTh StDev	0.07	0.79	P=0.45	P=0.22	P=0.57	P=0.31	P=0.61	P=0.79	P=0.85
	CoBMD Mean	0.06	0.85	P=0.56	P=0.37	P=0.96	P=0.78	P=0.88	P=0.99	P=0.95
	CoBMD Max	0.04	0.93	P=0.78	P=0.81	P=0.43	P=0.84	P=0.59	P=0.82	P>0.99
	CoBMD StDev	0.12	0.42	P=0.07	P=0.52	P=0.07	P=0.47	P=0.10	P=0.51	P=0.58
Lateral Tibia	CoTh Mean	0.09	0.66	P=0.55	P=0.57	P=0.64	P=0.75	P=0.86	P=0.72	P=0.57
	CoTh Max	0.18	0.14	P=0.67	P=0.54	P=0.61	P=0.78	P=0.41	P=0.62	P=0.46
	CoTh StDev	**0.30**	**0.008**	P=0.25	P=0.60	P=0.42	P=0.71	P=0.86	P=0.20	P=0.18
	CoBMD Mean	0.12	0.44	P=0.40	P=0.14	P=0.75	P=0.53	P=0.97	P=0.71	P=0.58
	CoBMD Max	0.10	0.58	P=0.48	P=0.36	P=0.98	P=0.68	P=0.79	P=0.75	P=0.63
	CoBMD StDev	0.19	0.12	P=0.05	P=0.57	P=0.01	P=0.99	P=0.02	P=0.08	P=0.17
Lateral Femur	CoTh Mean	0.07	0.81	P=0.62	P=0.51	P=0.33	P=0.70	P=0.46	P=0.86	P=0.81
	CoTh Max	0.17	0.18	P=0.23	P=0.52	P=0.32	P=0.98	P=0.34	P=0.97	P=0.97
	CoTh StDev	0.17	0.20	P=0.53	P=0.66	P=0.33	P=0.26	P=0.33	P=0.58	P=0.46
	CoBMD Mean	0.15	0.29	P=0.26	P=0.05	P=0.43	P=0.18	P=0.36	P=0.50	P=0.54
	CoBMD Max	0.06	0.81	P=0.61	P=0.56	P=0.27	P=0.88	P=0.32	P=0.45	P=0.39
	CoBMD StDev	0.09	0.63	P=0.94	P=0.83	P=0.15	P=0.77	P=0.19	P=0.32	P=0.34

Table S3. Results from multiple linear regression model with model fit, main effects, and interaction effects between age, sex, and rapamycin treatment are shown for subchondral cortical bone analyses. Co=cortical, Th=Thickness, BMD=bone mineral density. Relationships where P≤0.05 are highlighted in **red**, and trends where P≤0.1 but >0.05 are **bolded**. Individual main effect and interaction predictors are similarly highlighted upon significant model fit.

Variable		*Model Fit*		*Main Effects*			*2-way Interactions*			*3-way Interactions*
		R^2	P	Age	Sex	Treatment	Age x Sex	Age x Treatment	Sex x Treatment	Age x Sex x Treatment
MT	TbTh Mean	**0.21**	**0.08**	P=0.13	P=0.95	P=0.15	P=0.82	P=0.29	P=0.07	P=0.15
	Tb BVF	**0.11**	**0.08**	P=0.32	P=0.90	P=0.59	P=0.83	P=0.53	P=0.74	P=0.73
	TbBMD	**0.22**	**0.07**	**P=0.04**	P=0.67	P=0.27	P=0.86	P=0.45	P=0.25	P=0.60
MF	TbTh Mean	0.10	0.61	P=0.58	P=0.51	P=0.42	P=0.70	P=0.61	P=0.71	P=0.95
	Tb BVF	0.17	0.18	P=0.42	P=0.77	P=0.23	P=0.98	P=0.22	P=0.86	P=0.92
	Tb BMD	**0.34**	**0.002**	**P=0.002**	P=0.33	P=0.61	P=0.95	P=0.59	P=0.87	P=0.62
LT	TbTh Mean	**0.32**	**0.003**	P=0.39	P=0.67	**P=0.02**	P=0.73	**P=0.10**	P=0.15	P=0.10
	Tb BVF	0.11	0.54	P=0.99	P=0.36	P=0.14	P=0.38	P=0.17	P=0.28	P=0.28
	Tb BMD	0.13	0.38	P=0.26	P=0.88	P=0.92	P=0.60	P=0.67	P=0.81	P=0.38
LF	TbTh Mean	0.17	0.20	P=0.67	P=0.29	P=0.28	P=0.22	P=0.57	P=0.39	P=0.30
	Tb BVF	0.08	0.69	P=0.47	P=0.41	P=0.86	P=0.72	P=0.80	P=0.94	P=0.66
	Tb BMD	**0.29**	**0.01**	**P=0.05**	P=0.87	P=0.27	P=0.30	P=0.27	P=0.32	P=0.16

Table S4. Results from multiple linear regression model with model fit, main effects, and interaction effects between age, sex, and rapamycin treatment are shown for subchondral trabecular bone analyses. M=medial, L=lateral, T=tibia, F=femur, Tb=trabecular, Th=Thickness, BVF=bone volume fraction, BMD=bone mineral density. Relationships where P≤0.05 are highlighted in **red**, and trends where P≤0.1 but >0.05 are **bolded**. Individual main effect and interaction predictors are similarly highlighted upon significant model fit.

Variable		*Model Fit*		*Main Effects*			*2-way Interactions*			*3-way Interactions*
		R^2	P	Age	Sex	Treatment	Age x Sex	Age x Treatment	Sex x Treatment	Age x Sex x Treatment
WJ	Total	**0.24**	**0.02**	**P=0.002**	P=0.19	P=0.86	**P=0.04**	P=0.78	P=0.68	P=0.42
	ACS	**0.25**	**0.02**	**P=0.0009**	P=0.11	P=0.71	**P=0.03**	P=0.54	P=0.41	P=0.32
	PG	**0.20**	**0.07**	**P=0.006**	P=0.16	P=0.69	**P=0.05**	P=0.97	P=0.68	P=0.46
	CC	0.18	0.13	P=0.02	P=0.48	P=0.85	P=0.29	P=0.93	P=0.81	P=0.71
MT	Total	**0.30**	**0.004**	**P=0.002**	P=0.16	P=0.48	**P=0.06**	P=0.64	P=0.66	P=0.52
	ACS	**0.28**	**0.008**	**P=0.004**	P=0.24	P=0.51	P=0.12	P=0.63	P=0.77	P=0.67
	PG	**0.27**	**0.009**	**P=0.004**	P=0.25	P=0.64	**P=0.08**	P=0.80	P=0.50	P=0.36
	CC	**0.24**	**0.02**	**P=0.005**	P=0.25	P=0.64	**P=0.08**	P=0.80	P=0.50	P=0.36
MF	Total	**0.21**	**0.06**	**P=0.003**	P=0.22	P=0.80	**P=0.05**	P=0.81	P=0.58	P=0.95
	ACS	**0.29**	**0.004**	**P=0.003**	P=0.60	P=0.65	P=0.43	P=0.92	P=0.19	P=0.38
	PG	0.10	0.49	P=0.03	P=0.23	P=0.80	P=0.16	P=0.67	P>0.99	P=0.89
	CC	0.11	0.42	P=0.05	P=0.47	P=0.81	P=0.29	P=0.98	P=0.76	P=0.94
LT	Total	0.10	0.49	P=0.05	P=0.32	P=0.58	P=0.18	P=0.53	P=0.43	P=0.45
	ACS	0.19	0.10	P=0.01	P=0.08	P=0.19	P=0.07	P=0.28	P=0.11	P=0.21
	PG	0.12	0.37	P=0.04	P=0.22	P=0.78	P=0.10	P=0.74	P=0.66	P=0.47
	CC	0.06	0.85	P=0.61	P=0.82	P=0.70	P=0.84	P=0.65	P=0.96	P=0.86
LF	Total	**0.22**	**0.05**	**P=0.03**	P=0.62	P=0.16	P=0.14	P=0.59	P=0.66	P=0.87
	ACS	**0.24**	**0.02**	**P=0.03**	P=0.67	P=0.19	P=0.35	P=0.24	P=0.56	P=0.49
	PG	0.16	0.18	P=0.03	P=0.48	P=0.45	P=0.18	P>0.99	P=0.97	P=0.65
	CC	0.18	0.11	P=0.005	P=0.18	P=0.83	P=0.08	P=0.34	P=0.37	P=0.21

Table S5. Results from multiple linear regression model with model fit, main effects, and interaction effects between age, sex, and rapamycin treatment are shown for histological analyses for the whole-joint and individual compartments. WJ-whole joint, M=medial, L=lateral, T=tibia, F=femur. Relationships where P≤0.05 are highlighted in **red**, and trends where P≤0.1 but >0.05 are **bolded**. Individual main effect and interaction predictors are similarly highlighted upon significant model fit.

Table S6: microCT scoring system for radiographic evaluation of OA.

MicroCT Finding	**Score**
Osteophyte location	1 = medial/lateral tibia 2 = patella 3 = medial/lateral femur
Osteophyte size	0 = none 1 = small (<1mm) 3 = large (≥1mm)
Subchondral bone cystic changes	0 = no 1 = yes
Subchondral bone sclerosis	0 = no 1 = yes
Articular bone lysis	0 = no 1 = yes
Intra-articular soft tissue	0 = normal 1 = increased

Table S7: Grading criteria for histological evaluation of OA in marmosets.

Parameter	Grade	Description
Articular Cartilage Structure	0	Normal
	1	Undulating articular surface, but no fibrillation
	2	Mild superficial fibrillation involving < half of the plateau/condyle
	3	Mild superficial fibrillation involving > half of the plateau/condyle
	4	Mild fibrillation/clefts/loss involving up to 1/3 depth of articular cartilage thickness in < half of plateau/condyle
	5	Mild fibrillation/clefts/loss involving up to 1/3 depth of articular cartilage thickness in ≥ half of plateau/condyle
	6	Moderate fibrillation/clefts/loss involving up to 2/3 depth of articular cartilage thickness in < half of the plateau/condyle
	7	Moderate fibrillation/clefts/loss involving up to 2/3 depth of noncalcified articular cartilage thickness in & half of the plateau/condyle
	8	Severe fibrillation/clefts/loss involving > 2/3 depth of articular cartilage thickness in < half of plateau/condyle
	9	Severe fibrillation/clefts/loss involving > 2/3 depth of articular cartilage thickness in > half of plateau/condyle
	10	Clefts/loss of articular cartilage through tidemark
	11	Clefts/loss of articular cartilage through to subchondral bone
Tidemark Duplication	0	None (only one tidemark)
	1	2 tidemarks
	2	>2 tidemarks
	3	No visible tidemark remaining
Toluidine Blue Staining	0	Normal (no loss of staining in articular cartilage)
	1	Moderate loss of staining in up to 1/2 depth of articular cartilage thickness and involving < half of the plateau/condyle
	2	Moderate loss of staining in up to 1/2 depth of articular cartilage thickness involving > half of the plateau/condyle
	3	Moderate loss of staining in > 1/2 depth of articular cartilage thickness and involving < half of plateau/condyle

	4	Moderate loss of staining in > 1/2 depth of articular cartilage thickness and involving 2 half of plateau/condyle
	5	Severe loss of staining up to 1/2 depth of articular cartilage thickness and involving < half of plateau/condyle
	6	Severe loss of staining up to 1/2 depth of articular cartilage thickness and involving ≥ half of plateau/condyle
	7	Severe loss of staining in >1/2 depth of articular cartilage thickness and involving < half of the plateau/condyle
	8	Severe loss of staining in > 1/2 depth of articular cartilage thickness and involving ≥ half of plateau/condyle
Chondrocyte Cellularity	0	0-5 groupings of hypertrophic chondrocytes or chondrones containing <3 cells.
	1	6-10 groupings in chondrones or clusters containing 3 or more cells.
	2	>10 groupings of chondrones or clusters containing 3 or more cells.
	3	Loss of cellularity in <1/2 of the plateau or condyle.
	4	Loss of cellularity in 1/2 or greater of the plateau or condyle.

Table S8: Grading criteria for evaluation of synovium/joint capsule.

Parameter	Grade	Description
Pannus Infiltration	0	No pannus
	1	Pannus >2 cells thickness is present on the bone at the joint margin but has not migrated over the cartilage surface.
	2	Pannus has migrated over the cartilage surface OR invaded into the cartilage < 1x cartilage depth.
	3	Pannus has migrated over the cartilage surface OR invaded into the cartilage > 1x cartilage depth.
Bone Erosion	0	No cortical bone erosion at any site.
	1	Partial thickness loss of cortical bone only.
	2	Focal complete loss of cortical bone. Communication with the marrow cavity at only one small vascular communication site.
	3	Widespread complete loss of cortical bone. Multiple sites of communication with marrow cavity or broad area loss of cortical bone.
Synovial Hyperplasia	0	1 cell thick
	1	2-3 cells thick
	2	4-5 cells thick
	3	>5 cells thick
Sub-Synovial Inflammation	0	No inflammatory cells
	1	Occasional scattered inflammatory cells – perivascular or scattered throughout.
	2	Focal areas of dense sub-synovial white blood cell infiltrate but still predominantly normal sub-synovial areolar connective tissue present.
	3	Widespread dense sub-synovial white blood cell infiltrate. Markedly reduced or little/no normal areolar connective tissue OR lymphoid follicle formation – distinct accumulation of mononuclear cells organized into rounded masses reminiscent of lymph nodules.
Synovial Exudate	0	No inflammatory cells or fibrin in the synovial cavity.
	1	Inflammatory cells and/or fibrin clot in the synovial cavity.
Synovial/Joint Capsule Fibrosis (Severity)	0	< 1/3x cartilage thickness
	1	1/3-2/3x cartilage thickness but not densely packed fibrous tissue.
	2	1/3-2/3x cartilage thickness and densely packed fibrous tissue.
	3	2/3-1x cartilage thickness but not densely packed fibrous tissue.
	4	2/3-1x cartilage thickness and densely packed fibrous tissue.
	5	>1x cartilage thickness but not densely packed fibrous tissue.
	6	>1x cartilage thickness and densely packed fibrous tissue.

Synovial/Joint Capsule Fibrosis (Coverage)	0	<20%
	1	21-40%
	2	41-60%
	3	61-80%
	4	>80%

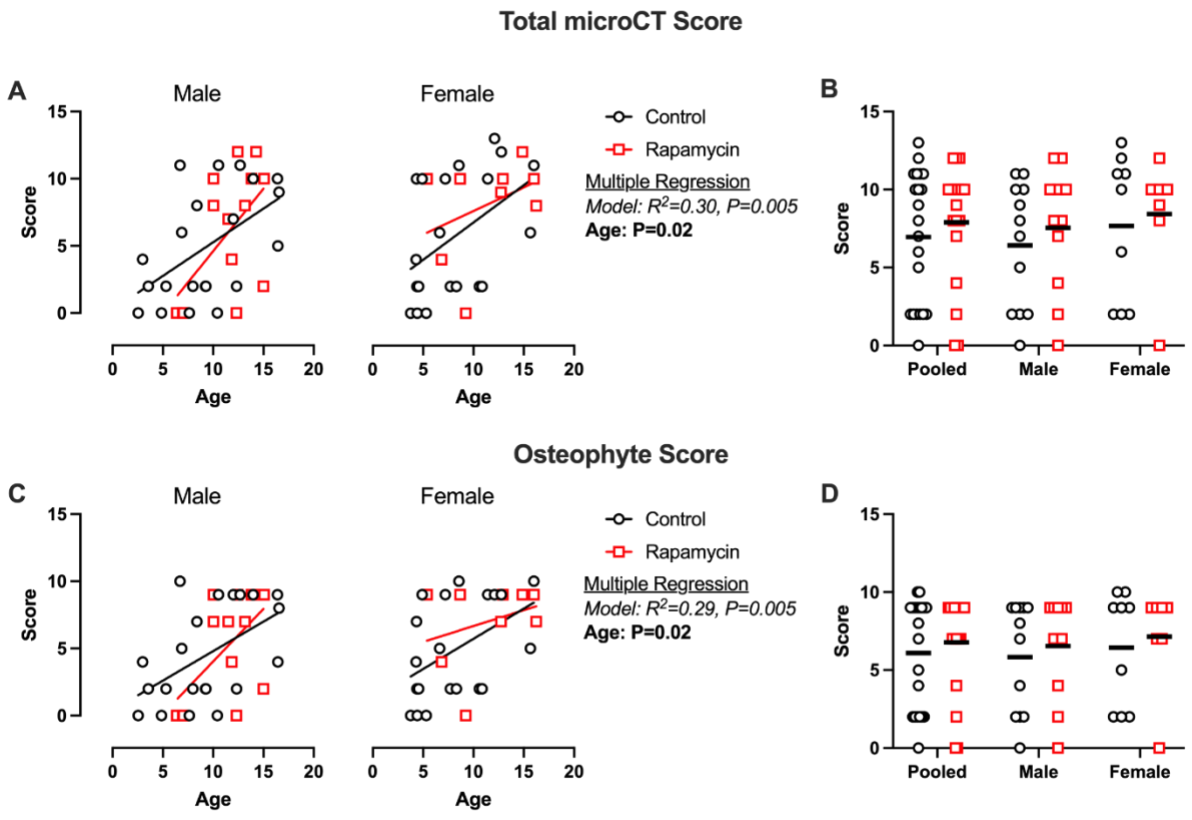

Figure S1: Radiographic OA is similar between control and rapamycin-treated marmosets. **A**) Total uCT OA scores presented as scatter plots against age and **B**) stratified by treatment group for geriatric males, females, and pooled sexes. **C**) Osteophyte scores are similarly presented as scatter plots against age and **D**) stratified by treatment group for geriatric males, females, and pooled sexes. Results of multiple linear regression (A,C) are shown beside graphs. Comparisons between groups were made using Mann-Whitney tests (B,D). Data are presented as mean with individual data points.

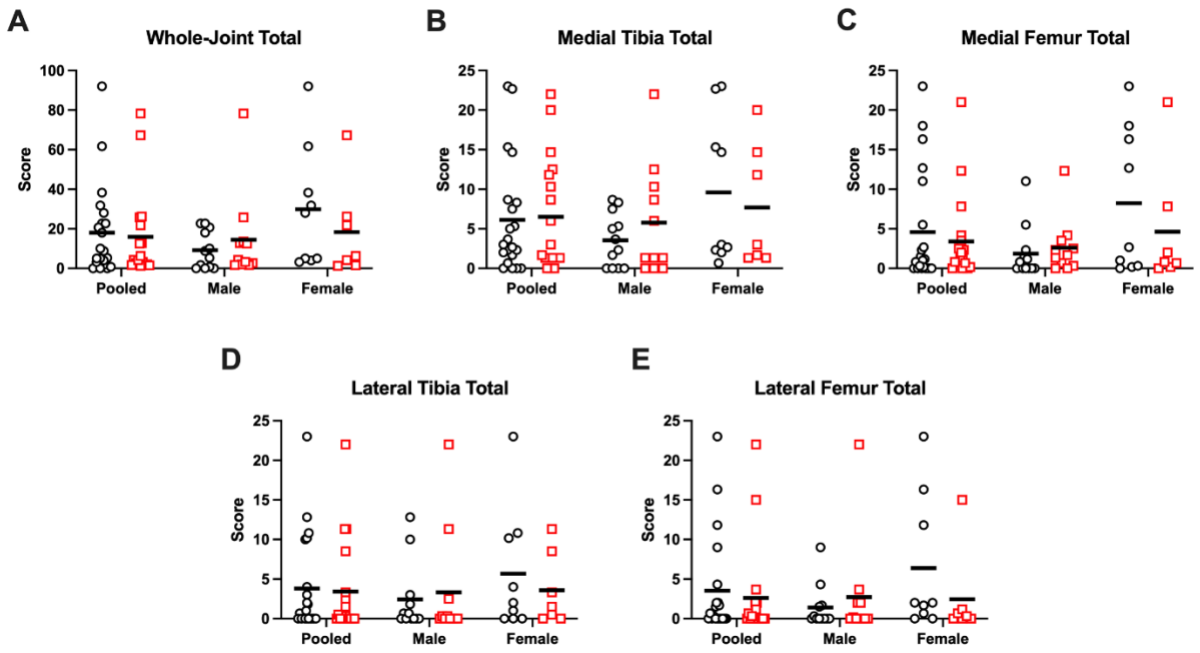

Figure S2: Cartilage histopathology was not affected by rapamycin. **A**) Total histological scores for the whole-joint, **B**) medial tibia and **C**) femur, and **D**) lateral tibia and **E**) femur are compared between control and rapamycin-treated geriatric marmosets when pooled and stratified by sex. Controls are presented as Comparisons were made using Mann-Whitney tests. Data are presented as mean with individual data points.

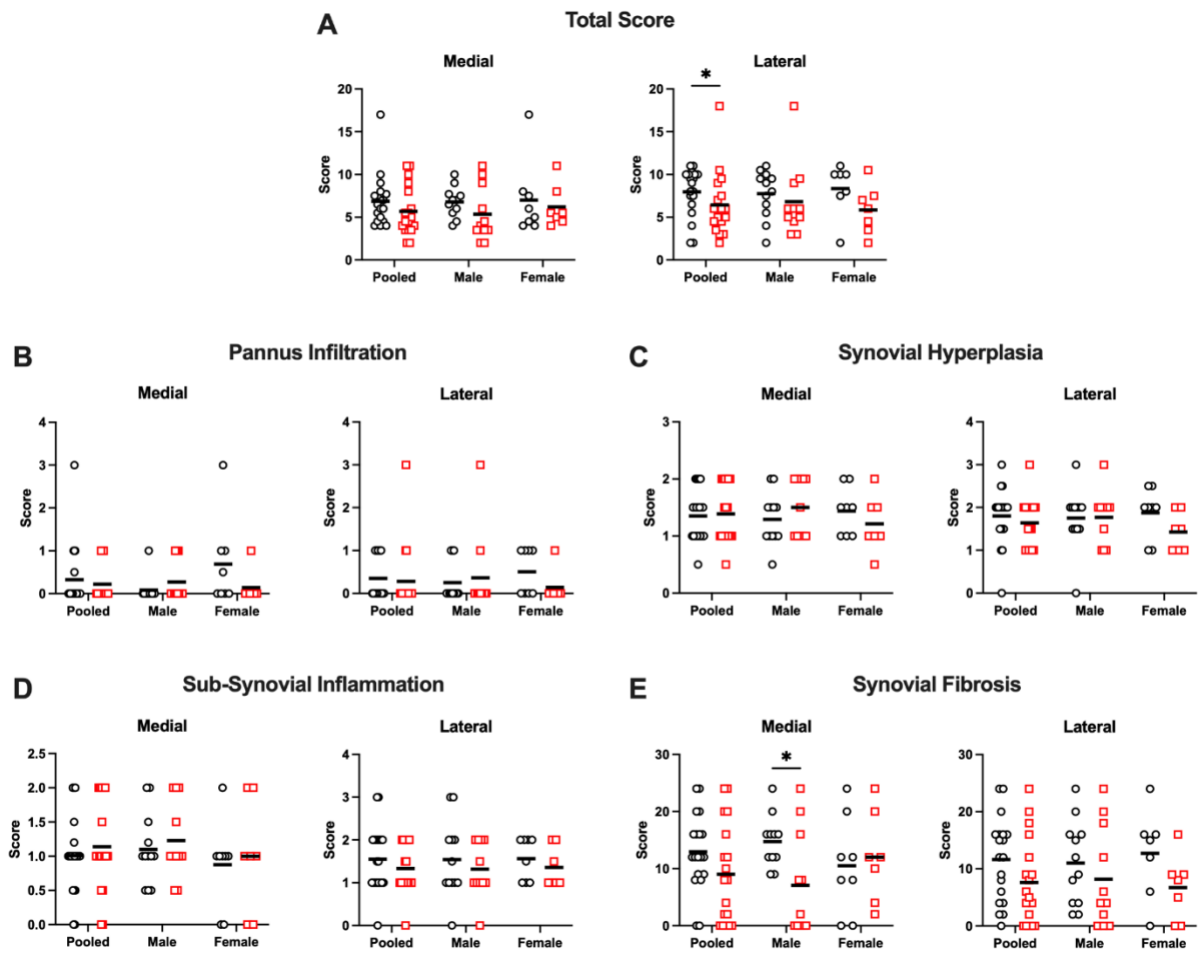

Figure S3: Effect of rapamycin on synovitis. **A**) Total synovial score and the individual scoring criteria of **B**) pannus infiltration, **C**) synovial hyperplasia, **D**) sub-synovial inflammation, and **E**) synovial fibrosis for the medial and lateral compartments are shown for geriatric control and rapamycin-treated marmosets pooled and stratified by sex. Comparisons were made using unpaired t-tests or Mann-Whitney tests, depending on normality of data. Data are presented as mean with individual data points. *P<0.05

References

1. Tardif S, Ross C, Bergman P, Fernandez E, Javors M, Salmon A, et al. Testing efficacy of administration of the antiaging drug rapamycin in a nonhuman primate, the common marmoset. J Gerontol A Biol Sci Med Sci. 2015 May;70(5):577–87.

2. Minton DM, Ailiani AR, Focht MDK, Kersh ME, Marolf AJ, Santangelo KS, et al. The common marmoset as a translational model of age-related osteoarthritis. GeroScience [Internet]. 2024 Mar 11 [cited 2024 Mar 20]; Available from: https://doi.org/10.1007/s11357-024-01103-5

3. Kobak KA, Batushansky A, Borowik AK, Lopes EPB, Peelor III FF, Donovan EL, et al. An In Vivo Stable Isotope Labeling Method to Investigate Individual Matrix Protein Synthesis, Ribosomal Biogenesis, and Cellular Proliferation in Murine Articular Cartilage. Function. 2022 Mar 23;3(2):zqac008.

4. Minton DM, Elliehausen CJ, Javors MA, Santangelo KS, Konopka AR. Rapamycin-induced hyperglycemia is associated with exacerbated age-related osteoarthritis. Arthritis Res Ther. 2021 Dec;23(1):253.

5. Ang IC, Fox M, Polk JD, Kersh ME. An Algorithm for Automated Separation of Trabecular Bone From Variably Thick Cortices in High-Resolution Computed Tomography Data. IEEE Transactions on Biomedical Engineering. 2020 Mar;67(3):924–30.

6. Radakovich LB, Marolf AJ, Shannon JP, Pannone SC, Sherk VD, Santangelo KS. Development of a microcomputed tomography scoring system to characterize disease progression in the Hartley guinea pig model of spontaneous osteoarthritis. Connective Tissue Research. 2018 Nov 2;59(6):523–33.

7. Furman BD, Strand J, Hembree WC, Ward BD, Guilak F, Olson SA. Joint degeneration following closed intraarticular fracture in the mouse knee: A model of posttraumatic arthritis. J Orthop Res. 2007 May;25(5):578–92.

8. Haubruck P, Heller R, Blaker CL, Clarke EC, Smith SM, Burkhardt D, et al. Streamlining quantitative joint-wide medial femoro-tibial histopathological scoring of mouse post-traumatic knee osteoarthritis models. Osteoarthritis and Cartilage. 2023 Dec 1;31(12):1602–11.